On-Line Measurement of Exhaled [^{11}C]CO_2 During PET

Roger N. Gunn, Alex Ranicar, Jeff T. Yap, Paula Wells, Safiye Osman, Terry Jones, and Vincent J. Cunningham

Medical Research Council Cyclotron Unit, Hammersmith Hospital, Imperial College School of Medicine, London, United Kingdom

The purpose of this study was to develop and evaluate a system for the continuous on-line measurement of expired $^{11}CO_2$ during ^{11}C PET studies. **Methods:** A detector system was developed that allowed continuous sampling of expired air during PET. Healthy volunteers (n = 4) underwent PET with [^{11}C]CO_2 during which expired air, tomographic tissue activity, and blood data were collected. The measured expired-air $^{11}CO_2$ radioactivity time courses were filtered, and an envelope was extracted and compared with the time course of $^{11}CO_2/H^{11}CO_3^-$ in blood. **Results:** Good agreement was found between the shapes of the expired-air envelope and the time course in blood, enabling quantitative calibration against discrete blood samples. **Conclusion:** A system for the continuous monitoring of expired radioactivity during PET has been developed and evaluated with [^{11}C]CO_2. This monitoring enables the quantitative continuous measurement of $^{11}CO_2/H^{11}CO_3^-$ in blood.

Key Words: [^{11}C]CO_2; PET; expired air; metabolites

J Nucl Med 2000; 41:605–611

An important consideration in the analysis of PET data is the formation in vivo of radiolabeled metabolites of the parent tracer. For ^{11}C-labeled tracers, CO_2 ($^{11}CO_2$) is probably the most commonly occurring metabolite (*1*). Exchange of $^{11}CO_2$ between plasma [^{11}C]bicarbonate ($H^{11}CO_3^-$) and expired air, although rapid, can nonetheless contribute significantly to the total radioactivity measured in blood and tissues throughout scanning. Thus, its retention and distribution in vivo must be taken into account in the quantitative analysis of many PET studies using ^{11}C-labeled tracers.

This article describes a simple method for continuous monitoring of $^{11}CO_2$ in expired air during PET. Further, a method of data analysis is described that relates the expired radioactivity to the corresponding concentration time course of $^{11}CO_2/H^{11}CO_3^-$ in arterial blood.

Monitoring of expired radioactivity during PET was introduced by Koeppe et al. (*2*) for the quantification of local cerebral blood flow using the inert, freely diffusible gaseous tracer [^{18}F]methyl fluoride. Their aim was to quantitate flow while avoiding arterial blood sampling, under the assumption that alveolar and end-expiratory gas concentrations are proportional to the arterial blood concentrations leaving the lungs.

Received Mar. 1, 1999; revision accepted Jul. 30, 1999.

For correspondence or reprints contact: Roger N. Gunn, PhD, Medical Research Council Cyclotron Unit, Hammersmith Hospital, Imperial College School of Medicine, DuCane Rd., London W12 0NN, UK.

This work was principally concerned with monitoring $^{11}CO_2$ as an endogenously produced metabolite of other parent tracers. Data from blood and exhaled air were obtained from a PET series during which healthy volunteers received intravenous bolus injections either of [^{11}C]bicarbonate or of 2-[^{11}C]thymidine (which is catabolized to $^{11}CO_2$). These scans form part of a study investigating the contribution of $^{11}CO_2/H^{11}CO_3^-$ to the tissue signal after 2-[^{11}C]thymidine administration (*3,4*).

MATERIALS AND METHODS

Radiochemicals

[^{11}C]CO_2 was produced by bombardment of nitrogen containing 1% O_2 with 19-MeV protons ($^{14}N(p,\alpha)^{11}C$). The gas was bubbled for approximately 2 min through a mixture of $NaHCO_3$ solution for injection (8.4% BP) diluted with isotonic saline (1:9, percent volume in volume). We prepared 2-[^{11}C]thymidine as described previously (*5*).

Healthy Volunteers

The data were taken from a study of 2-[^{11}C]thymidine uptake in tumors. The study were approved by the Research Ethics Committee of the Royal Postgraduate Medical School, Hammersmith Hospital. Permission to administer the radioactive tracers was obtained from the Administration of Radioactive Substances Advisory Committee of the United Kingdom.

PET was performed on a 931 ECAT camera (CTI/Siemens, Inc., Knoxville, TN). For both the [^{11}C]bicarbonate scans (514 MBq) and the 2-[^{11}C]thymidine scans (487 MBq), the tracer was administered as a 30-s intravenous bolus.

Assay of $^{11}CO_2$ in Expired Air

Healthy volunteers wore a loose-fitting single-use nasal oxygen set (Portex, Hythe, UK) (Fig. 1A) connected to a scintillation detector by polytetrafluoroethylene tubing (length, 150 cm; internal diameter, 2.5 mm). They were asked to breathe normally through the nose. Air was drawn from the nasal set through the detector using a nonpulsatile air pump (Dymax 30; Charles Austin Pumps Ltd., Byfleet, UK) set at 1.5 L/min. The air line was also sampled downstream of the detector through a capnograph (model 455; P.K. Morgan Ltd., Gillingham, UK) at a rate of 0.25 L/min.

In adults with a ventilation rate of 5–7 L/min, this device clearly does not collect the full volume of expired air. Rather, the device samples the concentration of radioactivity in the inspired and expired air and, hence, requires calibration. With a collection rate of 1.5 L/min, the air in the detector chamber is replaced at a rate of about 7 Hz. This sampling rate is sufficient to characterize the respiratory cycle.

Scintillation Detector

The scintillation detector was constructed of type 412 scintillating plastic (Bicron, Newbury, OH) and is shown in Figures 1B and

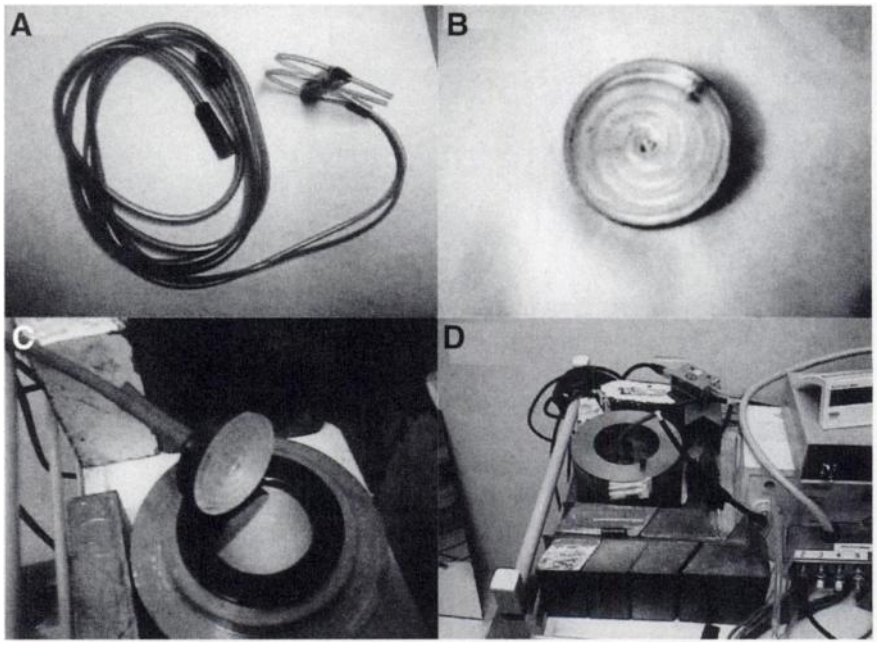

FIGURE 1. Photographs show parts of expired-air monitoring system, including nasal oxygen set (A), spiral chamber (B), spiral chamber and single photomultiplier tube (C), and scintillation detection unit and lead shielding (D).

C. The air was drawn through a spiral chamber (total volume, 3.34 mL) cut in the plastic, with a 2-mm plastic lid sealed with optical cement, to give 4π geometry. The internal dimensions of the spiral cut were 2.5 mm wide and 4.5 mm deep, leaving a wall thickness of 2 mm. The spiral design was chosen to promote effective flushing of air in the detector. The inside of the spiral was coated with a 500-Å film of Parylene (Nova Tran Ltd., Northampton, UK) to minimize diffusion of $^{11}CO_2$ into the plastic. The device was covered with Teflon tape (DuPont, Wilmington, DE) backed with light-tight black tape and was bonded to the face of a single 9957B bialkali photomultiplier tube (Thorn EMI CRL, London, UK) (Fig. 1C) using a BC-634a optical coupling (Bicron). Figure 1D shows the final assembly with lead shielding. Output from the photomultiplier was preamplified (Ortec 113; EG & G Instruments, Wokingham, UK) and fed to an Ortec ACE Mate amplifier and single-channel analyzer (EG & G). The device was primarily sensitive to positrons. The mean energy of positrons arising from the decay of ^{11}C was 394 keV, with a maximum of 970 keV. At first, an ungated energy spectrum up to approximately 1000 keV was obtained; subsequently, a lower energy window was set to exclude noise in the spectral region less than 15 keV. Data were logged at intervals of 0.1 s on a personal computer with a timer–counter card (DPC-10; Blue Chip Technology, Clwyd, UK) using software developed in-house.

The sensitivity of the system was determined by cross-calibration against a high-pressure ion chamber. A known volume (5–10 mL) of $[^{11}C]CO_2$ gas was drawn into a syringe, and the total activity was measured in an ion chamber. This gas was then mixed with 1 L air in a nonpermeable gas bag, from which the detector was flushed and filled. The system was then closed for calibration and dead-time measurements. The dead time of the system was estimated from the apparent decay in the counting rate of ^{11}C from a maximum of 120,000 observed counts/s over a period of 3 h. Over this long, static period, a small loss of gas from the detector was apparent, because the terminal decay rate was slightly greater than the isotopic decay rate. We assumed that this loss was caused by the permeability of the apparatus and tubing to gas. The static data were therefore analyzed in terms of a nonparalyzable model incorporating a leakage term,

$$C_{true}(t) = A_0 \times \exp(-(\lambda + \rho) \times t) + C_{back}$$

$$C_{obs}(t) = C_{true}(t)/(1 + D \times C_{true}(t)),$$

where $C_{true}(t)$ (counts/s) denotes the true counting rate in the field of view at time t (s), A_0 (counts/s) denotes the true counting rate of the radioisotope at time $t = 0$, C_{back} (counts/s) denotes the background counting rate, λ (0.0005663/s) denotes the fractional decay rate of ^{11}C, $C_{obs}(t)$ (counts/s) denotes the observed counting rate, D (s/count) denotes the nonparalyzable dead time per observed count, and ρ (s^{-1}) denotes the apparent loss of gas from the system over the 3-h period.

A weighted nonlinear least-squares fit of the model parameters (A_0, ρ, D) to the data ($C_{obs}(t)$) was obtained using a simplex algorithm (*6*). Weights were set in inverse proportion to $C_{obs}(t)$. The dead time of the system as configured above was $4.75 \pm 0.17 \times 10^{-6}$ s/count (mean [±SD] of 4 estimates), with a value for ρ of $4.76 \pm 0.72 \times 10^{-5}$/s. (i.e., a half-life of 243 min). In dynamic use, the system operates under a slightly negative pressure with a short transit time (7 Hz); any loss attributable to gas leakage in dynamic use would therefore be vanishingly small.

The 4π geometry and spiral construction of the chamber enable it to detect positrons resulting from the decay of ^{11}C in air with great efficiency (92%). Its relatively low efficiency in detecting 511-keV γ radiation results in a low background count during scanning.

Assay of Radioactivity and $^{11}CO_2/H^{11}CO_3^-$ in Blood

Total radioactivity in arterial blood was also assayed continuously on-line throughout scanning. A radial artery was cannulated, and blood was withdrawn at a rate of 2.5 mL/min through a bismuth germanium oxide γ detector using a method that has been described in detail (*7*). In addition, discrete samples of blood were taken from the line at intervals for calibration against a well counter and for the assay of $^{11}CO_2/H^{11}CO_3^-$ and of other radiolabeled metabolites of the parent tracers. The line was flushed intermittently with heparinized saline.

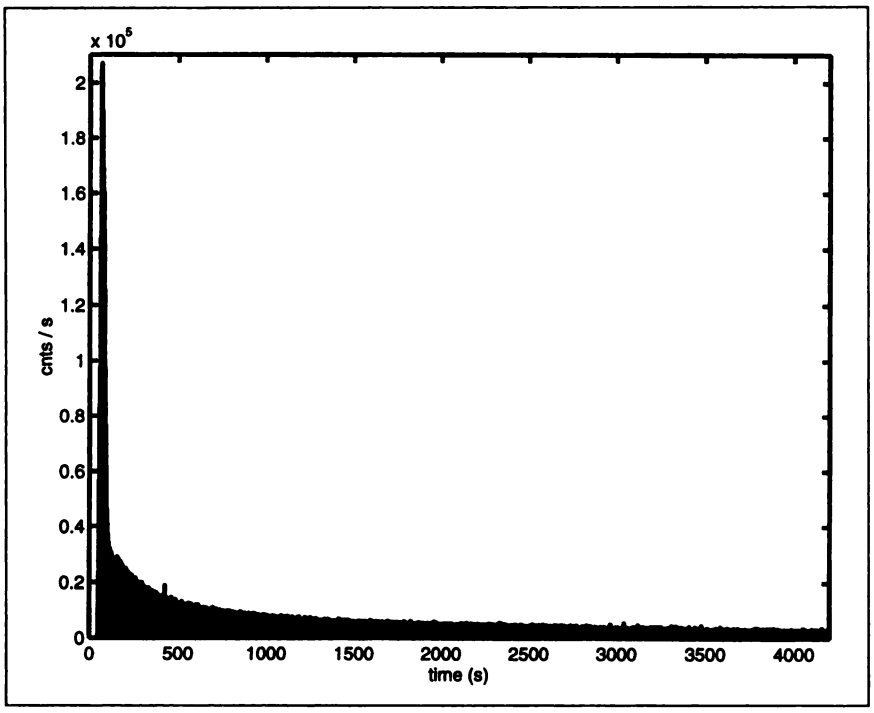

FIGURE 2. Recording of exhaled $^{11}CO_2$ after intravenous bolus injection of [^{11}C]bicarbonate. cnts = counts.

$^{11}CO_2/H^{11}CO_3^-$ was measured in the discrete blood samples using, essentially, a previously described method (*8*). Aliquots (0.2 mL) of blood were immediately added to tubes containing 0.8 mL sodium hydroxide (0.5 mol/L) and capped to trap the radioactive CO_2. Another aliquot (0.2 mL) of blood was added to 0.6 mL isopropanol, followed by 0.2 mL hydrochloric acid (0.5 mol/L). Nitrogen gas was bubbled through this mixed sample to expel the radioactive CO_2. Radioactivity in the aliquots was then measured in a γ counter (Compugamma 1282; LKB/Pharmacia, Uppsala, Sweden).

RESULTS

A typical example of the time course of exhaled $^{11}CO_2$ after intravenous bolus injection of [^{11}C]bicarbonate, and measured as described above, is shown in Figure 2. An expanded detail of the time course of the exhaled $^{11}CO_2$ is shown in Figure 3, in which the respiratory oscillations in the raw data are clearly defined. Inspection of this type of data suggests that the envelope of the total data set, which corresponds to end-expiratory gas concentra-

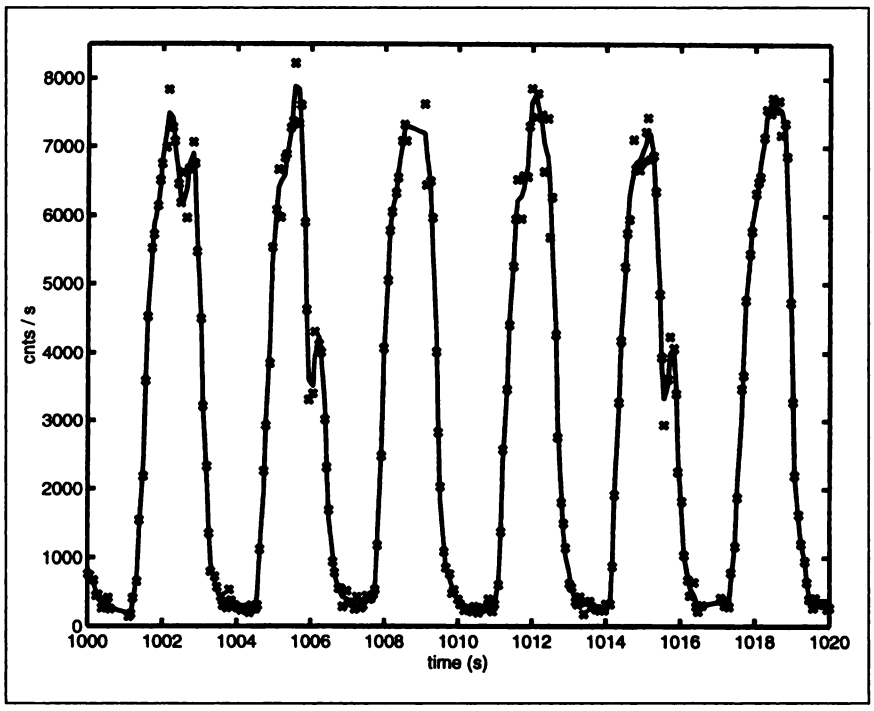

FIGURE 3. Segment of Figure 2 shows time course of exhaled $^{11}CO_2$ (x) and associated low-pass filtered data (continuous line). cnts = counts.

tions (compare Koeppe et al. (2)), may provide a suitable description and measure of the corresponding time course of the concentration of $^{11}CO_2/H^{11}CO_3^-$ in the blood.

The data were first characterized by examining power spectral density (9). The power spectrum corresponding to the exhaled $^{11}CO_2$ data in Figures 2 and 3 is shown in Figure 4. The power spectrum yields 2 important pieces of information. First, the power of the signal in this example drops markedly above 2 Hz, suggesting that appropriate smoothing could be performed using a low-pass filter with a cutoff frequency of 2 Hz. A fourth-order Butterworth filter was applied, and the smoothed time course is shown as the solid line in Figure 3. This procedure allows the peak value of each breath to be used as a more robust measure of the envelope describing the concentration of radioactivity in the end-expired air. Second, the maximum energy of the signal occurs at a frequency of approximately 0.2 Hz, corresponding to an average respiratory cycle (rc) of 5 s. This length was used as a window with which to search the filtered data for maxima. Once a maximum has been found at time (t), the next maximum is obtained in the interval [t + rc/2, t + 3 rc/2]. The resultant envelope for this example is shown in Figure 5.

The relationship between the envelope of exhaled $^{11}CO_2$ and the concentration of $^{11}CO_2/H^{11}CO_3^-$ in arterial blood was examined using data from [^{11}C]bicarbonate scanning during which both expired air and blood had been sampled continuously. The percentage of total radioactivity in discrete blood samples that was attributable to $^{11}CO_2/H^{11}CO_3^-$ after intravenous administration of [^{11}C]bicarbonate is shown in Table 1 and was more than 90% throughout the scans. Similar figures have been reported for dogs (82%–95% after 60 min) (1). A linear interpolated fit to this data was used to correct the continuously sampled on-line blood data and give a continuous time course of $^{11}CO_2/H^{11}CO_3^-$ in arterial blood. The plasma-to-blood ratio of the radioactivity was constant throughout scanning, with a mean (±SD) of 1.17 ± 0.04 (n = 4 scans). These discrete blood samples also allow absolute calibration of the blood data against a well counter and, hence, against the PET camera (6).

To compare the time–activity curve of radioactivity in exhaled air with that in blood, the envelope was scaled such that the integral from 5 min to the end of scanning was equal to that of the corresponding time course of the $^{11}CO_2/H^{11}CO_3^-$ arterial blood curve. Figure 6 shows an example of the match after intravenous administration of [^{11}C]bicarbonate. Initially, the exhalation curve is higher than the blood curve, but after a few minutes the shapes of the curves are well matched. Similar results were obtained in all instances in which [^{11}C]bicarbonate was administered as an intravenous bolus.

After intravenous injection of 2-[^{11}C]thymidine, $^{11}CO_2$ was again detected in the breath almost immediately, reflecting the whole-body catabolism of the parent tracer (8). Figure 7 shows a typical example of the percentage of total radioactivity in arterial blood attributable to $^{11}CO_2/H^{11}CO_3^-$, as measured in discrete blood samples. These data were fitted to an equation of the form

$$F(t) = \begin{cases} t \le d, & 0 \\ t > d, & \alpha(1 - e^{-\beta(t-d)}), \end{cases}$$

where F denotes the fraction of $^{11}CO_2/H^{11}CO_3^-$ in blood and α, β, and d (delay) are the parameters to be estimated.

The primary purpose of this fit was to interpolate these data from 5 min to the end of discrete CO_2 sampling (15 min) so as to scale the expired-air envelope to the product of

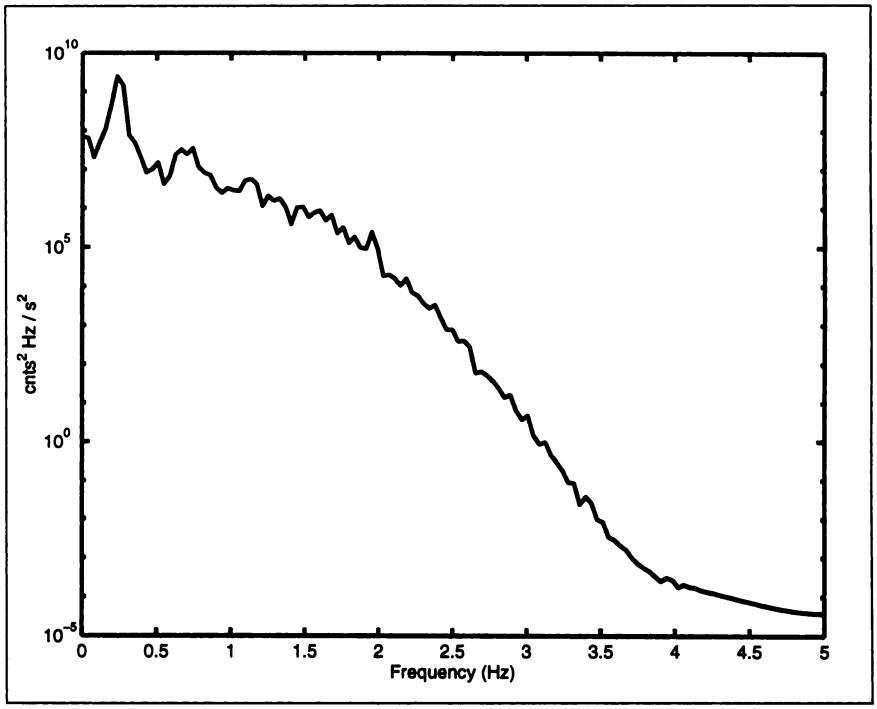

FIGURE 4. Power spectrum corresponds to exhaled $^{11}CO_2$ data in Figures 2 and 3. cnts = counts.

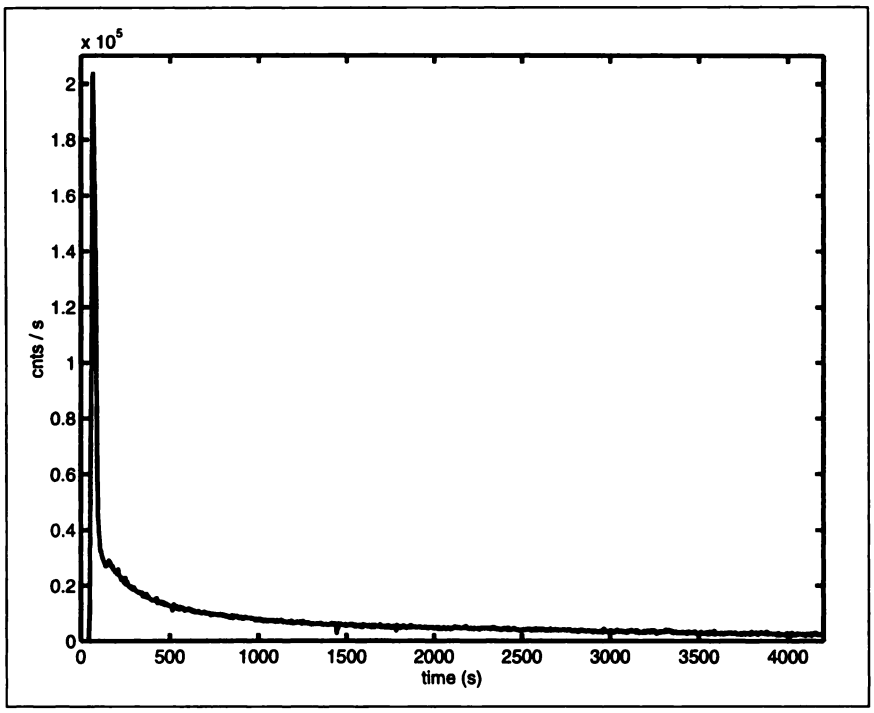

FIGURE 5. Envelope of exhaled $^{11}CO_2$ curve obtained after filtering raw data shown in Figure 2 and finding local peaks. cnts = counts.

F and the measured total activity in blood over the same period. This process gives an estimate of the concentration time course of $^{11}CO_2/H^{11}CO_3^-$ derived from 2-[^{11}C]thymidine in arterial blood (Fig. 8). The extrapolated portion of the fit (Fig. 7) is used simply for illustration to extend the comparison of an extrapolated estimate of $^{11}CO_2/H^{11}CO_3^-$ in blood to the end of scanning (Fig. 8).

Again, in this case, in which $^{11}CO_2$ derives from endogenous catabolism of the parent tracer, the scaled exhalation envelope is initially slightly higher than the blood envelope. However, a close match between the exhalation curve and the arterial blood curve is obtained after a few minutes.

DISCUSSION

This article describes a simple and highly sensitive device for the continuous detection of radioactivity in exhaled air from individuals undergoing PET. The study was principally concerned with detection of radiolabeled CO_2 as a metabolite of ^{11}C-labeled tracers and the relationship between activity in exhaled air and that in blood. We intend to use such data to correct for the contribution of $^{11}CO_2/H^{11}CO_3^-$ to the tissue signal measured by PET, as is described in an accompanying paper (*4*). The device may also facilitate other applications in PET, such as the measurement of tissue pH, because the partitioning of CO_2 between plasma and tissue depends on pH (*10*).

TABLE 1
$^{11}CO_2/H^{11}CO_3^-$ in Blood After Intravenous Bolus Injection of [^{11}C]bicarbonate in 4 Studies

Time after injection (s)	$^{11}CO_2/H^{11}CO_3^-$ ± SD (%)
0	100
100	99.6 ± 0.3
300	97.9 ± 0.8
640	96.1 ± 2.6
1800	92.2 ± 3.9
3600	89.3 ± 4.7

The sensitivity of the detector is illustrated by the clearness of the respiratory cycle, as is apparent in the raw data sampled at 10 Hz. In the application we are studying, this sensitivity is important because it allows sufficient temporal sampling to define the respiratory peaks of the end-expired air after filtering of the raw data. Sufficient sampling, in turn, allows use of a robust envelope of the curve to relate the concentration of radioactivity in expired air to that in blood.

Because the expired radioactivity is only sampled rather than fully recovered, absolute quantitative studies in PET require cross-calibration with the blood. We cross-calibrated by scaling the integrals of the time–activity curves of the end-expired air and of $^{11}CO_2/H^{11}CO_3^-$ in blood. The capnograph in the system can also allow the specific activity of the expired CO_2 to be used to cross-calibrate against total CO_2/HCO_3 in blood.

The tissue signal in PET is usually characterized and modeled relative to an input function defined from arterial blood or plasma. Expired air, however, reflects mixed arteriovenous blood. The consequent difference between the shapes of the time–activity curves in expired air and in arterial blood is apparent soon after intravenous bolus injection of [^{11}C]bicarbonate. An analogous difference occurs for endogenously produced $^{11}CO_2$ arising from the in vivo metabolism of parent ^{11}C-labeled tracers, as we show for 2-[^{11}C]thymidine. The difference in shape at early times,

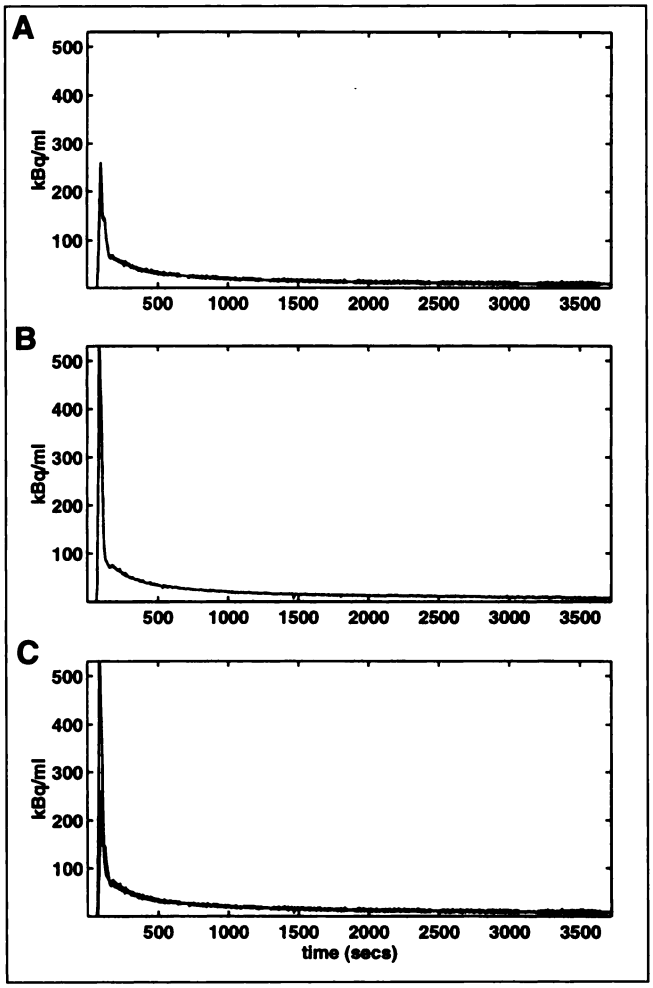

FIGURE 6. Typical example of time course of $^{11}CO_2/H^{11}CO_3^-$ in blood (A) and calibrated envelope of expired air (B) after intravenous administration of [^{11}C]bicarbonate. (C) Superimposition of the 2 curves.

however, is less apparent because of the relatively slower evolution of $^{11}CO_2/H^{11}CO_3^-$, and again, a subsequent concordance was seen between the shapes of the time–activity curves in blood and expired air after a short period. These initial differences can be attributed to a first-pass effect. At early times, $^{11}CO_2/H^{11}CO_3^-$ in venous blood is exchanged and distributed in lung interstitial fluid and alveolar gas, resulting in an initial unidirectional loss of tracer as measured in the arterial blood. Later, an effective secular equilibrium exchange is established, resulting in close concordance of the shapes in venous blood, expired air, and arterial blood.

In the study by Koeppe et al. (*2*), cross-calibration of the expired radioactivity with the corresponding arterial blood concentrations was possible using discrete venous blood samples. Koeppe et al. point out that because the tracer [^{18}F]methyl fluoride is inert and freely diffusible, the integrals of the venous and arterial blood activity time courses should be equal. Because the scanning period was short, equilibrium between arterial and venous concentrations was not reached. A compartmental model was therefore used to relate venous blood and expired air and to calibrate the system. In general, for endogenously produced metabolites such as $^{11}CO_2/H^{11}CO_3^-$, the venous and arterial integrals will differ, and calibration against discrete arterial or arterialized venous samples may therefore be necessary.

In this study, discrete arterial blood samples were taken for the assay of the fraction of total radioactivity in blood recovered as $^{11}CO_2/H^{11}CO_3$. Scaling of the continuous exhalation data to blood was based on integrals derived from fits to the discrete blood data and from the corresponding continuously sampled total blood activity. The match between the shapes of the time–activity curves for blood and

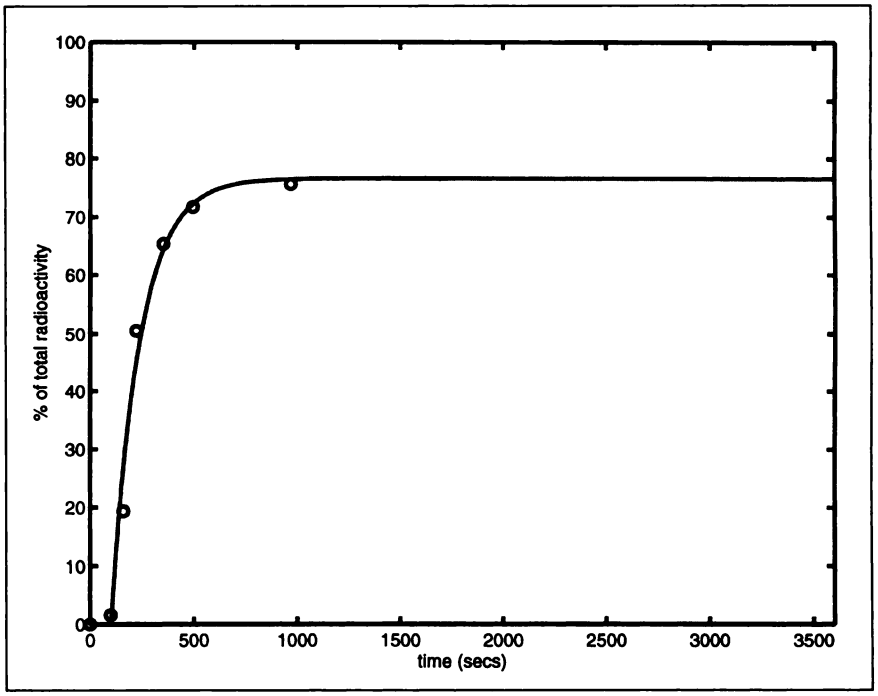

FIGURE 7. Percentage of total radioactivity in arterial blood attributable to $^{11}CO_2/H^{11}CO_3^-$ after intravenous administration of 2-[^{11}C]thymidine. Data were fitted (continuous line) to functional form involving time delay followed by exponential approach to constant value. Extrapolated portion is for illustration only.

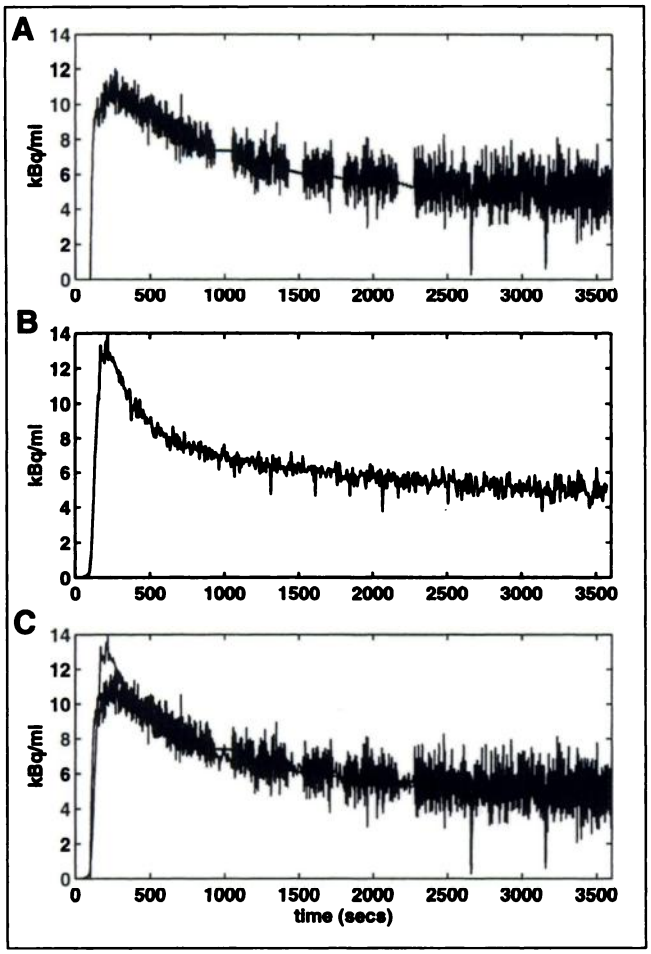

FIGURE 8. Typical example of time course of $^{11}CO_2/H^{11}CO_3^-$ in blood (A) and calibrated envelope of expired air (B) after intravenous administration of 2-[^{11}C]thymidine. (C) Superimposition of the 2 curves.

expired air does, however, indicate that scaling could be performed on the basis of a few discrete blood samples taken in the mid to later parts of scanning.

In general, continuous measures make best use of the available signal, and continuous monitoring of expired air has several clear advantages in the generation of input functions for quantitative analysis. For rapid changes, the definition and execution of an appropriate rapid, discrete blood sampling protocol may be difficult. Continuous sampling avoids the need for a functional form or model to interpolate and extrapolate discrete data samples across the entire scanning period. A major advantage is the sensitivity of the system. A marked improvement in signal-to-noise ratio is apparent in the envelope of the expired radioactivity compared with the blood data, as Figures 6 and 8 illustrate.

CONCLUSION

During PET, the exhaled-air scintillation detector we have described can, with high sensitivity and fine temporal resolution, monitor the in vivo production of $^{11}CO_2$ arising from metabolism of ^{11}C-labeled parent tracer.

REFERENCES

1. Shields AF, Graham MM, Kozawa SM, et al. Contribution of labeled carbon dioxide to PET imaging of carbon-11-labeled compounds. *J Nucl Med.* 1992;33: 581–584.
2. Koeppe RA, Holden JE, Polcyn RE, et al. Quantitation of local cerebral blood flow and partition coefficient without arterial sampling: theory and validation. *J Cereb Blood Flow Metab.* 1985;5:214–223.
3. Gunn RN. *Mathematical Modelling and Identifiability Applied to Positron Emission Tomography Data* [dissertation]. Warwick, UK: University of Warwick; 1996.
4. Gunn RN, Yap JT, Wells P, et al. A general method to correct PET data for tissue metabolites using a dual-scan approach. *J Nucl Med.* 2000;41:706–711.
5. Steel CJ, Brady F, Luthra SK, et al. An automated radiosynthesis of 2-[^{11}C]thymidine using anhydrous [^{11}C]urea derived from [^{11}C]phosgene. *Appl Radiat Isot.* 1999;51:377–388.
6. Nelder JA, Mead R. A simplex method for function minimization. *Comput J.* 1965;7:308–313.
7. Ranicar ASO, Williams CW, Schnorr L, et al. The on-line monitoring of continuously withdrawn arterial blood during PET studies using a single BGO/photomultiplier assembly and non-stick tubing. *Med Prog Technol.* 1991;17: 259–264.
8. Shields AF, Mankoff D, Graham MM, et al. Analysis of 2-carbon-^{11}thymidine blood metabolites in PET imaging. *J Nucl Med.* 1996;37:290–296.
9. Oppenheim AV, Schafer RW. *Discrete-Time Signal Processing.* Englewood Cliffs, NJ: Prentice Hall; 1989:311–312.
10. Brooks DJ, Beaney RP, Thomas DGT, Marshall J, Jones T. Studies on regional cerebral pH in patients with cerebral tumours using continuous inhalation of $^{11}CO_2$ and positron emission tomography. *J Cereb Blood Flow Metab.* 1986;6:529–535.